J. Fluid Mech. (1974), *vol.* 63, *part* 3, *pp.* 509–527
Printed in Great Britain

Near-resonant forcing in a shallow two-layer fluid: a model for the internal surge in Loch Ness?

By S. A. THORPE
Institute of Oceanographic Studies, Wormley, Godalming, Surrey

(Received 13 July 1973)

The form taken by a finite amplitude internal seiche in a shallow two-layer fluid within a long narrow container is akin to a shock wave in a gas-filled tube; an undular bore or surge is present which reflects back and forth along the length of the container. The internal surge in Loch Ness is sometimes observed to retain its amplitude over several seiche periods, and a resonance with the wind appears possible. This idea is explored by developing a theoretical model and by making a laboratory experiment, but difficulties are encountered in estimating the size of the parameters which characterize the natural phenomenon.

1. Introduction

The set of equations which describes a given physical phenomenon can seldom be solved analytically, even when approximations are made or when the solution is required only over a restricted range of the parameters which characterize the phenomenon. The usual approach to such problems is to find, if possible, numerical solutions using a computer. An alternative method, which is sometimes possible, is to model the phenomenon on a laboratory scale. Both methods of approach suffer the disadvantage of producing solutions only for a finite set of values of the parameters. The latter method is often severely limited by the impossibility of properly reproducing simultaneously all the parameters which are important. It has, however, the advantage of sometimes revealing physical processes which have been overlooked in the mathematical formulation, or may, once the important parameters have been discovered, give some useful extension of the solution beyond the range for which solutions are possible by other means. This is an account of an attempt to model the internal surge in Loch Ness by a laboratory experiment, and describes how we were eventually foiled in completely achieving our objective by the problem of properly assessing the important features of the forcing mechanism.

The oscillations of the thermocline of Loch Ness (figure 1) were probably the first large-scale naturally occurring internal waves to be observed and investigated in detail. Watson (1904) was the first to interpret the observed oscillations as an internal seiche, and later detailed observations by Wedderburn (1907) showed that Watson's analysis was basically correct.† The loch is about 35 km

† Watson and Wedderburn's explanation of the oscillations evoked such scepticism at the time that Wedderburn was persuaded to prove the existence of internal seiches elsewhere, and this he did in the Madusee in Northern Germany (Wedderburn 1911).

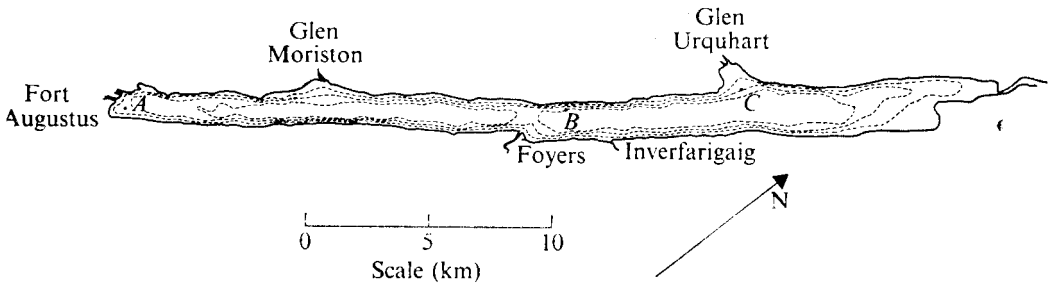

FIGURE 1. Loch Ness. The depth contours are at 200, 400 and 600 ft.

in length and 1·4 km wide, and has a mean depth of about 140 m. It is remarkably straight, lying in the Great Glen along the line of a fault, and is roughly oriented in the direction of the dominant winds. In early October there is a thermocline at a depth of about 40 m. It is 10–20 m thick, separating the warmer, about 12 °C, surface water from the colder, 6 °C, bottom water of the loch. The period of the fundamental internal seiche is about 52 h, corresponding to the first internal wave mode, with a wavelength twice the length of the loch. One puzzling observation of Wedderburn's was that, half-way along the loch near Inverfarigaig, waves were observed which had a period of about half that of the fundamental seiche. Wedderburn's observations were made with reversing thermometers (except for the occasional use of a platinum resistance thermometer, which produced evidence of thermal microstructure and pre-dated the discovery of thermocline fine structure by almost half a century), but Mortimer (1955) brought into use a thermistor chain and was able to obtain almost continuous records of the loch temperatures at nine fixed depths. He showed that the effect of the earth's rotation on the seiche is to produce a transverse tilt of the thermocline, and confirmed Watson's conclusion that the seiche could be generated by the wind. The seiche could easily be detected as long as a week after its generation. Watson and Mortimer's interpretation of the generation process is that the stress produced by strong winds blowing along the loch causes a transport of warmer surface water towards one end of the loch, where the thermocline is depressed, and when the wind falls the tendency of the thermocline to recover a level position initiates the seiche. Mortimer recognized that a complex circulation developed in the surface layers during wind forcing. (Heaps & Ramsbottom (1966) have made a theoretical study of this circulation.)

A surprising and persistent feature in Mortimer's observations was the sudden temperature increases which were observed at fixed levels at the south-west end of the loch during part of the seiche cycle (figure 2). These are not consistent with Watson's explanation of the seiche (based on linear theory), nor do they appear in theoretical and laboratory models of short internal standing waves (Thorpe 1968*a*). A well-known feature of long waves, however, is their tendency to steepen, and Mortimer's observations have been interpreted as being due to an internal surge or bore, which is the form taken by internal waves of given ampli-

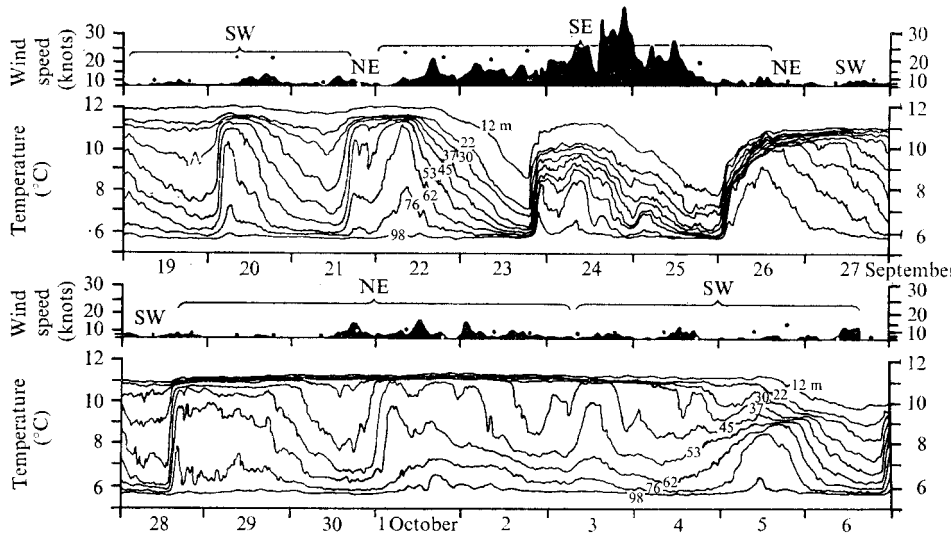

FIGURE 2. Temperature variation at fixed depths at A, see figure 1, near Fort Augustus, taken from Mortimer (1955). The solid black curves show the wind speed measured at Fort Augustus Abbey tower, plotted on a square-law scale.

tude and sufficiently great length†. Our observations (Thorpe 1971; Thorpe, Hall & Crofts 1972) have substantiated this conclusion. The seiche is a nonlinear phenomenon, akin to a tidal bore or shock wave, with a front which travels back and forth along the length of the loch. Its presence explains the half-period oscillation observed by Wedderburn. The rise in temperature observed at fixed depths as the surge passes is the result of an abrupt lowering of the thermocline, often by 10 m or more, and the long-wave theory of Long (1972) provides an explanation of this wave form. Cavanie (1971) has examined the development of an initial discontinuity in thermocline level, and his results show how the surge may develop from an initial wind-tilted thermocline as in Mortimer's model.

Often, after a strong wind, a surge will develop and travel a few times along the loch, becoming smaller as it does so. There are times however when the amplitude of the surge does not diminish, and it appears possible that the surge is then in resonance with the wind. Figure 3 shows the temperature measured every 15 min at a depth of 49·5 m at a position B, see figure 1, some 2 km from the centre of the loch from 10 to 20 October 1971 (when recording ended). An asymmetric oscillation with a period of about 26 h can be seen. The surge front is marked by arrows labelled NE and SW which indicate the directions of the advance of the surge. The oscillation is more fully resolved in figure 4, which shows the records of temperature at six levels at a position about one-quarter of the way down the loch from the north-east end (C, figure 1). The north-eastward-going surge passing the recorders soon after 06.00 h on 17 October is undular in form

† Similar internal bores have been observed in the Straits of Gibraltar by Ziegenbein (1969), in Massachusetts Bay by Halpern (1971), in the Straits of Georgia by Gargett & Hughes (1972) and in Seneca Lake by Hunkins & Fliegel (1973). The cause of the latter is unknown.

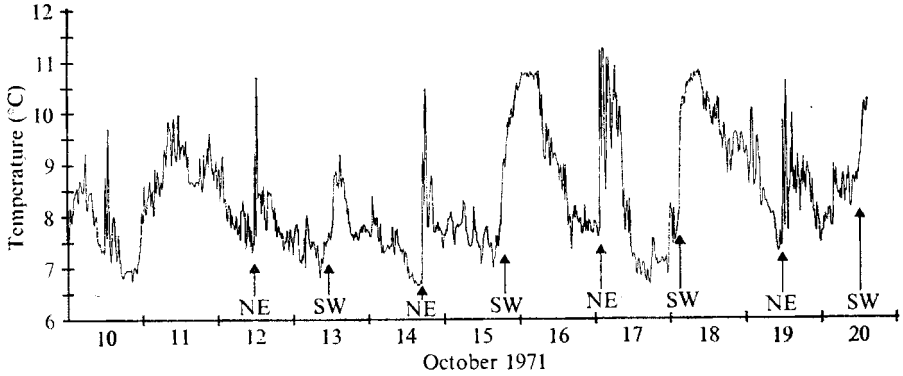

FIGURE 3. The temperature measured every 15 min at 49·5 m depth at *B*, see figure 1. The direction of advance of the surge (known from simultaneous measurements at *C*) is to the north-east (NE) or south-west (SW).

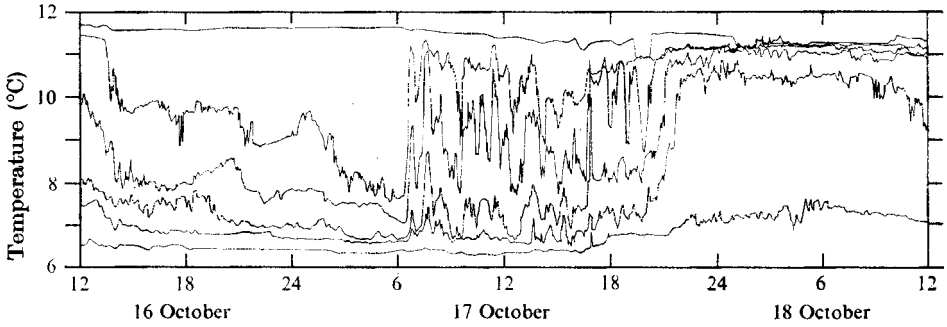

FIGURE 4. The temperature measured by thermistors at position *C*, see figure 1, and recorded every 2 min. The depths of the thermistors are 23, 43, 48, 53, 58 and 78 m.

with waves of period about 40 min. The reflected surge some 14 h later is more dispersed and does not appear to have an undular form. The waves are probably dissipated by reflexion at the rather irregular and gently sloping north-east end of the loch. The first three or four waves following a north-eastward-going surge are usually quite regular (more so than in figure 4), but they then become less coherent with higher frequencies appearing. This series of surges began after south-west winds† of about 12 m s^{-1} which lasted from the early morning of the 10th until the afternoon of the 11th. The following three days were calm but on the 15th and the 16th south-west winds of up to 8 m s^{-1} were recorded. The evening of the 16th was calm, but on the 17th and 18th the south-west wind again strengthened to speeds of 11 m s^{-1} in mid-loch. The wind fell on the evening of the 18th but rose once more during the daylight hours of the 19th, again from the south-west. The measurements of wind which are available for the period show that a *regular* forcing at the period of the surge is absent. There is, however, a significant south-west component with a period *near* the surge period, with an amplitude of about 4 m s^{-1}, superimposed on a mean speed of about the same magnitude, and a partial resonance appears possible.

† Winds were measured using cup anemometers from a cabin cruiser between *B* and *C*, figure 1.

In the following section we shall describe a model for periodic wind forcing of the loch, a model which closely corresponds to a laboratory experiment (§4). A two-layer model is considered, and an analogy is found between this and a single-layer fluid with a free surface, for which some solutions and experimental results are already available. We shall investigate the form taken by the surge and its dependence on the relevant parameters, and in particular we shall determine how close the forcing frequency must be to the natural frequency of oscillation for a surge to be generated. How well we are able to model the actual motions in the loch is discussed in §3.

2. Theory of resonant forcing

2.1. *The model*

We shall consider in this section a rectangular tank with vertical walls and ends which contains two layers of incompressible fluid, the upper of depth h_1 and density ρ_1, the lower of depth h_2 and density ρ_2 ($> \rho_1$). For simplicity we assume that the upper fluid is bounded above by a rigid horizontal plane, so that the only mode of oscillation possible is interfacial, in which the boundary between the two layers is set into motion. The fluids are subjected to a horizontal body force $F(z,t)$ per unit mass (the axis z is vertically upwards), acting along the length l of the tank in the direction of the x axis. The motion is assumed to lie in the x, z plane. The bottom of the tank is at $z = 0$, the top at $z = h_1 + h_2 = D$ and the ends are at $x = 0$, l. This model corresponds closely to the laboratory experiments which will be described in §4.

The method of analysis follows closely that described by Chester (1968) in his study of long surface waves in a container which is subjected to small horizontal oscillations at a frequency near that of the free waves. The analysis here is abbreviated with reference to Chester's work where possible. Chester's results were compared with experiments made by Chester & Bones (1968) with favourable agreement, in that the predicted wave forms were similar to those observed. This lends credence to the validity of the long-wave approximation which we shall employ.

2.2. *Governing equations*

Let the subscript i following variables refer to the upper ($i = 1$) or lower ($i = 2$) fluid layer. The depths are h_i and the velocities are $(u_i, 0, w_i)$. From the continuity equation and the boundary conditions

$$w_1 = 0 \quad \text{at} \quad z = D, \quad w_2 = 0 \quad \text{at} \quad z = 0,$$

we find that

$$\frac{\partial h_2}{\partial t} + \frac{\partial}{\partial x}(h_2 \overline{u}_2) = 0, \quad \frac{\partial h_2}{\partial t} - \frac{\partial}{\partial x}(h_1 \overline{u}_1) = 0, \tag{1}$$

where

$$\overline{u}_1 = \frac{1}{h_1}\int_{h_1}^{D} u_1 dz, \quad \overline{u}_2 = \frac{1}{h_2}\int_{0}^{h_2} u_2 dz.$$

Hence we find that

$$\partial(h_1 \overline{u}_1 + h_2 \overline{u}_2)/\partial x = 0, \tag{2}$$

and the total horizontal flux is a function of time only, and is zero if the ends of the tank do not move horizontally.

Integration of the horizontal component of the equations of motion leads to the pair of equations

$$\frac{\partial}{\partial t}(h_1\bar{u}_1)+\frac{\partial}{\partial x}\int_{h_2}^{D}u_1^2\,dx=-\frac{h_1}{\rho_1}\frac{\partial p_1}{\partial x}(h_2)-gh_1\frac{\partial h_2}{\partial x}+\chi_1+\int_{h_2}^{D}F(z,t)\,dz+S_1, \tag{3}$$

$$\frac{\partial}{\partial t}(h_2\bar{u}_2)+\frac{\partial}{\partial x}\int_{0}^{h_2}u_2^2\,dx=-\frac{h_2}{\rho_2}\frac{\partial p_2}{\partial x}(h_2)-gh_2\frac{\partial h_2}{\partial x}-\chi_2+\int_{0}^{h_2}F(z,t)\,dz+S_2 \tag{4}$$

(see Chester 1968), where p_i is the pressure, S_i represents terms due to viscous dissipation in the boundary layers at the walls, and which are discussed below, and

$$\chi_1=\int_{h_2}^{D}\frac{\partial}{\partial x}\left\{\int_{h_2}^{z}\left(\frac{\partial w_1}{\partial t}+u_1\frac{\partial w_1}{\partial x}+w_1\frac{\partial w_1}{\partial z}-\nu_1\nabla^2 w_1\right)dz_1\right\}dz, \tag{5}$$

$$\chi_2=\int_{0}^{h_2}\frac{\partial}{\partial x}\left\{\int_{z}^{h_2}\left(\frac{\partial w_2}{\partial t}+u_2\frac{\partial w_2}{\partial x}+w_2\frac{\partial w_2}{\partial x}-\nu_2\nabla^2 w_2\right)dz_1\right\}dz. \tag{6}$$

Now since the pressure is continuous at the interface,

$$\partial p_1(h_2)/\partial x=\partial p_2(h_2)/\partial x,$$

and eliminating the terms containing the pressure gradient, we obtain from (3) and (4)

$$\frac{\rho_1}{h_1}\left\{\frac{\partial}{\partial t}(h_1\bar{u}_1)+\frac{\partial}{\partial x}\int_{h_2}^{D}u_1^2dz\right\}-\frac{\rho_2}{h_2}\left\{\frac{\partial}{\partial t}(h_2\bar{u}_2)+\frac{\partial}{\partial x}\int_{0}^{h_2}u_2^2dz\right\}=g(\rho_2-\rho_1)\frac{\partial h_2}{\partial x}$$
$$+\frac{\rho_1\chi_1}{h_1}+\frac{\rho_2\chi_2}{h_2}+\frac{\rho_1}{h_1}\int_{h_2}^{D}F(z,t)\,dz-\frac{\rho_2}{h_2}\int_{0}^{h_2}F(z,t)\,dz+\frac{\rho_1S_1}{h_1}-\frac{\rho_2S_2}{h_2}. \tag{7}$$

Equations (7) and (1) with the condition $h_1+h_2=D$ are used to specify the flow. Equation (7) is still exact and we now consider approximations, which may be justified *a posteriori*, appropriate to long interfacial waves. We suppose that the term

$$\frac{\partial}{\partial x}\int_{h_2}^{D}u_1^2dz$$

is small in comparison with $\partial(h_1\bar{u}_1)/\partial t$ and that it can be approximated by the expression $\partial(h_1\bar{u}_1^2)/\partial x$. Similarly

$$\frac{\partial}{\partial x}\int_{0}^{h_2}u_2^2dz$$

is approximated by $\partial(h_2\bar{u}_2^2)/\partial x$. The term χ_1 is approximated by

$$\int_{h_2}^{D}\frac{\partial}{\partial x}\left\{\int_{h_2}^{z}\frac{\partial w_1}{\partial t}dz_1\right\}dz$$

and χ_2 by

$$\int_{0}^{h_2}\frac{\partial}{\partial x}\left\{\int_{z}^{h_2}\frac{\partial w_2}{dt}dz_1\right\}dz.$$

These approximations are valid provided that both $\bar{u}_1$ and $\bar{u}_2$ are small in comparison with the speed of the propagating surge and that the deviations from the

mean flow in any cross-section are small, other than in the viscous boundary layers at the walls of the tank. The viscous terms in χ_1 will be important only in the side- and end-wall boundary layers and, being proportional to the vertical velocity, are much less than the viscous terms in S_1 and S_2 considered below. The solution which we shall find will be an approximation subject to these conditions, and these will impose a severe restriction upon the scale of waves which may be found to follow the surge front.

We shall suppose for simplicity that $F(z,t)$ is uniform in each layer and is periodic with frequency σ, so that

$$F(z,t) = \begin{cases} A_1 \cos \sigma t, & h_2 < z < D, \\ A_2 \cos \sigma t, & 0 < z < h_2, \end{cases}$$

where A_1 and A_2 are constants. (Chester had no such body force in his problem and the motion was induced by a horizontal motion of the end walls of the tank.) Equation (7) may now be reduced to the form

$$\rho_1 \frac{\partial \bar{u}_1}{\partial t} - \rho_2 \frac{\partial \bar{u}_2}{\partial t} - g(\rho_2 - \rho_1) \frac{\partial h_2}{\partial x} + (\rho_2 A_2 - \rho_1 A_1) \cos \sigma t = \left[\rho_2 \bar{u}_2 \frac{\partial \bar{u}_2}{\partial x} - \rho_1 \bar{u}_1 \frac{\partial \bar{u}_1}{\partial x} \right]$$
$$+ \left[\frac{\rho_1}{h_1} \int_{h_2}^{D} \frac{\partial}{\partial x} \left\{ \int_{h_2}^{z} \frac{\partial w_1}{\partial t} dz_1 \right\} dz + \frac{\rho_2}{h_2} \int_{0}^{h_2} \frac{\partial}{\partial x} \left\{ \int_{z}^{h_2} \frac{\partial w_2}{\partial t} dz_1 \right\} dz \right] + \left[\frac{\rho_1 S_1}{h_1} - \frac{\rho_2 S_2}{h_2} \right]. \tag{8}$$

The terms on the left side of this equation represent those which would be retained in a linear inviscid analysis. The three square brackets on the right represent the effects of finite amplitude, dispersion and dissipation respectively.

2.3. *The linear inviscid solution*

We consider first the solution obtained by neglecting the terms on the right-hand side of (8) and by adopting conventional series expansions

$$\bar{u}_i = u_i^{(1)} + u_i^{(2)} + \ldots, \quad h_i = h_i^{(0)} + h_i^{(1)} + h_i^{(2)} + \ldots, \tag{9}$$

where $h_1^{(0)}$ and $h_2^{(0)}$ are the mean depths of the upper and lower layers respectively, so that $h_1^{(0)} + h_2^{(0)} = D$. Retaining the leading terms of these series in the equations we find from (1), (2) and (8)

$$\rho_1 \frac{\partial u_1^{(1)}}{\partial t} - \rho_2 \frac{\partial u_2^{(1)}}{\partial t} - g(\rho_2 - \rho_1) \frac{\partial h_2^{(1)}}{\partial x} = (\rho_1 A_1 - \rho_2 A_2) \cos \sigma t, \tag{10}$$

$$\partial h_2^{(1)} / \partial t + h_2^{(0)} \partial u_2^{(1)} / \partial x = 0 \tag{11}$$

and

$$h_1^{(0)} u_1^{(1)} + h_2^{(0)} u_2^{(1)} = 0. \tag{12}$$

These may be combined to give the pair of equations

$$\frac{\partial u}{\partial t} + a_0 \frac{\partial a}{\partial x} = \beta \cos \sigma t, \quad \frac{\partial a}{\partial t} + a_0 \frac{\partial u}{\partial x} = 0,$$

where

$$\left.\begin{aligned} a_0^2 &= \frac{g(\rho_2-\rho_1)\,h_1^{(0)}h_2^{(0)}}{\rho_1 h_2^{(0)}+\rho_2 h_1^{(0)}}, \quad u_1^{(1)} = -\frac{a_0 u}{h_1^{(0)}}, \quad u_2^{(1)} = \frac{a_0 u}{h_2^{(0)}}, \\ h_1^{(1)} &= -h_2^{(1)} = a, \quad \beta = \frac{\rho_2 A_1 - \rho_1 A_2}{g(\rho_2-\rho_1)}\,a_0. \end{aligned}\right\} \tag{13}$$

Here a_0 is the speed of long free progressive waves of small amplitude at the interface. A solution which satisfies the boundary condition $u_1^{(1)} = u_2^{(1)} = 0$ at $x = 0$ is

$$u = \frac{\beta}{\sigma}\sin\sigma t\left(\cos\frac{\sigma x}{a_0} - 1\right) + h_1^{(0)}\left[f\left(t-\frac{x}{a_0}\right) - f\left(t+\frac{x}{a_0}\right)\right], \tag{14}$$

$$a = -\frac{\beta}{\sigma}\cos\sigma t\sin\frac{\sigma x}{a_0} + h_1^{(0)}\left[f\left(t+\frac{x}{a_0}\right) + f\left(t-\frac{x}{a_0}\right)\right], \tag{15}$$

where f is an arbitrary function. (We have scaled f so that $h_1^{(1)} = 2h_1^{(0)}f(t)$ at $x = 0$.) If this function f is chosen so that the boundary conditions at $x = l$ are also satisfied then we find

$$u = \frac{\beta}{\sigma}\sin\sigma t\left[\frac{\cos\left[\sigma(l-2x)/2a_0\right]}{\cos\left(\sigma l/2a_0\right)} - 1\right], \tag{16}$$

which is singular when the fluid is forced near resonance by a body force of frequency σ close to a natural frequency $(2m-1)\pi l/a_0$ (m is an integer) of the tank. We avoid this singularity by introducing higher order terms. The function f is not yet specified in (14) and (15). Near resonance f will dominate in the expressions for u and a, and we shall therefore proceed to solve the second-order equations with u and a (and therefore $u_i^{(1)}$ and $h_i^{(1)}$) represented by the terms in f alone and seek a solution which is valid near resonance and which, at this higher order, satisfies the boundary conditions at both $x = 0$ and $x = l$. We must first return to (8) and cast the dispersion and dissipation terms into convenient forms.

Following Chester we write the dispersive term occurring in (8) in the form

$$-a_0^2\frac{\rho_1 h_1^{(0)}+\rho_2 h_2^{(0)}}{\pi h_2^{(0)3}}\int_{-\infty}^{\infty}\frac{\partial}{\partial x}\left[h_2^{(1)}(x-\zeta,t) - h_2^{(1)}(x,t)\right]\log\tanh\frac{\pi|\zeta|}{4h_2^{(0)}}\,d\zeta. \tag{17}$$

The effects of viscous dissipation are, we shall suppose, limited to the regions at the walls of the tank and at the interface between the fluids. The dissipative term is

$$\frac{\rho_1 S_1}{h_1} - \frac{\rho_2 S_2}{h_2} = \frac{\rho_1\nu_1}{h_1 b}\int_{h_2}^{D}\int_0^b \nabla^2 u_1\,dy\,dz - \frac{\rho_2\nu_2}{h_2 b}\int_0^{h_2}\int_0^b \nabla^2 u_2\,dy\,dz, \tag{18}$$

where b is the width of the tank, ν_i is the kinematic viscosity and the y-integration is over the width. To a good approximation

$$\frac{\rho_1 S_1}{h_1} - \frac{\rho_2 S_2}{h_2} = \frac{2\tau_1^{(1)}}{b} + \frac{\tau_1^{(2)}}{h_1^{(0)}} + \frac{\tau_1^{(3)}}{h_1^{(0)}} - \frac{2\tau_2^{(1)}}{b} - \frac{\tau_2^{(2)}}{h_2^{(0)}} - \frac{\tau_2^{(3)}}{h_2^{(0)}}, \tag{19}$$

where $\tau_i^{(1)}$ is the stress on the walls in the x direction per unit area, $\tau_i^{(2)}$ is the stress per unit area on the horizontal boundary to the fluid and $\tau_i^{(3)}$ is the stress per unit area at the interface.

We write the shear stress in the form

$$\rho_i \left(\frac{\nu_i}{\pi}\right)^{\frac{1}{2}} \int_0^\infty \frac{\partial}{\partial t} u_i(x, t-\zeta)\, \zeta^{-\frac{1}{2}}\, d\zeta$$

and the expression for the dissipative terms takes the form

$$2\left(\frac{\nu_2}{\pi}\right)^{\frac{1}{2}} \rho_2 \left(\frac{1}{b}+\frac{1}{h_2^{(0)}}\right) \int_0^\infty \frac{\partial}{\partial t} u_2^{(1)}(x, t-\zeta)\, \zeta^{-\frac{1}{2}}\, d\zeta$$
$$-2\left(\frac{\nu_1}{\pi}\right)^{\frac{1}{2}} \rho_1 \left(\frac{1}{b}+\frac{1}{h_1^{(0)}}\right) \int_0^\infty \frac{\partial}{\partial t} u_1^{(1)}(x, t-\zeta)\, \zeta^{-\frac{1}{2}}\, d\zeta.$$

2.4. *Second-order solution*

We may now substitute the dispersive and dissipative terms into (8). We combine this equation with the equations of continuity (1) and (2), all expanded to second order, by making the transformation

$$U = \gamma_1 u_1^{(2)} + \gamma_2 u_2^{(2)}$$

(where γ_1 and γ_2 are constants; the details are given in the appendix) to obtain the pair of equations

$$(\partial/\partial t \pm a_0 \partial/\partial x)\,(U + h_2^{(2)}) = (\text{sum of terms containing products}$$
$$\text{of } f(t+x/a_0), f(t-x/a_0) \text{ and their derivatives; see equation (A 8)}).$$

These equations are now integrated and added to give an expression for U, and so, using (2), for $u_1^{(2)}$ and $u_2^{(2)}$. These satisfy the boundary condition $u_1^{(2)} = u_2^{(2)} = 0$ at $x = 0$, and we now impose the boundary condition $\gamma_1 \bar{u}_1 + \gamma_2 \bar{u}_2 = 0$ at $x = l$ to find the function f. Correct to second order

$$\gamma_1 \bar{u}_1 + \gamma_2 \bar{u}_2 = \gamma_1 u_1^{(1)} + \gamma_2 u_2^{(1)} + U$$
$$= \frac{\rho_2 A_2 - \rho_1 A_1}{\sigma g(\rho_2 - \rho_1)} a_0 \sin \sigma t \left(\cos \frac{\sigma x}{a_0} - 1\right) + h_1^{(0)} \left[f\left(t - \frac{x}{a_0}\right) - f\left(t + \frac{x}{a_0}\right)\right] + U, \tag{20}$$

using (14) and (A 7). At $x = l$ the expression is simplified by observing that, for a forcing frequency which is close to a natural frequency of the tank,

$$\sigma l/a_0 - (2m+1)\pi = \tan(\sigma l/a_0), \tag{21}$$

approximately. We impose now the condition that f shall be periodic (we are looking for a periodic solution) with period $2\pi(2m+1)/\sigma$, and (21) can be used to show that

$$f\left(t + \frac{l}{a_0}\right) = f\left(t - \frac{l}{a_0}\right) + \frac{2}{\sigma} \tan\left(\frac{\sigma l}{a_0}\right) f'\left(t - \frac{l}{a_0}\right),$$

approximately. Using this equation to simplify the expression for U at $x = l$, we find, retaining only the most significant terms,

$$\gamma_1\bar{u}_1+\gamma_2\bar{u}_2 \equiv \frac{a_0(\rho_2A_2-\rho_1A_1)}{\sigma g(\rho_2-\rho_1)}\sin\sigma t\left(\cos\frac{\sigma l}{a_0}-1\right)-\frac{2h_1}{\sigma}\tan\frac{\sigma l}{a_0}f'\left(t-\frac{l}{a_0}\right)$$
$$+\frac{3h_1 l}{a_0}\frac{(\rho_2h_1^2-\rho_1h_2^2)}{h_2(\rho_1h_2+\rho_2h_1)}f\left(t-\frac{l}{a_0}\right)f'\left(t-\frac{l}{a_0}\right)-\frac{lh_1^2}{\tau a_0h_2^2}\int_{-\infty}^{\infty}\left\{f'\left(t-\frac{l}{a_0}+\frac{\zeta}{a_0}\right)\right.$$
$$\left.-f'\left(t-\frac{l}{a_0}\right)\right\}\log\tanh\frac{\pi|\zeta|}{4h_2}\,d\zeta-\frac{2lh_1^2h_2}{(\rho_1h_2+\rho_2h_1)a_0}$$
$$\times\left[\left(\frac{\nu_1}{\pi}\right)^{\frac{1}{2}}\rho_1\left(\frac{1}{b}+\frac{1}{h_1}\right)+\left(\frac{\nu_2}{\pi}\right)^{\frac{1}{2}}\rho_2\left(\frac{1}{b}+\frac{1}{h_2}\right)\right]\int_0^{\infty}f'\left(t-\frac{l}{a_0}-\zeta\right)\zeta^{-\frac{1}{2}}\,d\zeta=0 \tag{22}$$

at $x = l$, where we have dropped the superscript (0) from h_1 and h_2. This equation has the same form as was found by Chester. So that a direct comparison with his numerical results may be made we shall forfeit some of the symmetry which might be exploited. With the substitution $\sigma t = 2\tau$, $f(t) = \epsilon_1^{\frac{1}{2}}F(\tau)$, equation (22) may be integrated to give

$$c+\tfrac{1}{2}\cos 2\tau = \{\operatorname{sgn}[\rho_2h_1^2-\rho_1h_2^2]\}F^2-\frac{4r}{\pi}F+\frac{4r^2}{\pi}$$
$$-\frac{4}{3\pi\delta\epsilon^{\frac{1}{2}}}\int_{-\infty}^{\infty}(F(\tau-\zeta)-F(\tau))\log\tanh\left(\frac{\pi|\zeta|}{2\delta}\right)d\zeta-\left(\frac{2}{\pi}\right)^{\frac{1}{2}}s\int_0^{\infty}F(\tau-\zeta)\zeta^{-\frac{1}{2}}\,d\zeta, \tag{23}$$

where c is a constant,

$$\epsilon=\frac{4}{3}\frac{a_0^2(\rho_1A_1-\rho_2A_2)}{g(\rho_2-\rho_1)\sigma_2^2}\left|\frac{1-\cos(\sigma l/a_0)}{\cos(\sigma l/a_0)}\right|\frac{h_2|\rho_2h_1^2-\rho_1h_2^2|}{h_1^3l(\rho_1h_2+\rho_2h_1)}$$

and

$$\epsilon_1=\frac{\epsilon h_1^2(\rho_1h_2+\rho_2h_1)^2}{(\rho_2h_1^2-\rho_1h_2^2)^2},\quad r=\frac{\pi}{3}\frac{h_2a_0}{h_1l\sigma\epsilon^{\frac{1}{2}}}\tan\frac{\sigma l}{a_0},$$

$$\delta=\frac{\sigma h_2}{a_0},\quad s=\frac{4}{3}\frac{h_2^2}{\epsilon^{\frac{1}{2}}\sigma^{\frac{1}{2}}(\rho_1h_2+\rho_2h_1)}\left[\frac{\nu_1^{\frac{1}{2}}\rho_1}{h_1}\left(\frac{1}{b}+\frac{1}{h_1}\right)+\frac{\nu_2^{\frac{1}{2}}\rho_2}{h_2}\left(\frac{1}{b}+\frac{1}{h_2}\right)\right],$$

and we have chosen the x direction so that $\rho_1A_1-\rho_2A_2 \geqslant 0$.

Equation (23) is identical to Chester's equation (5.22) if $\operatorname{sgn}[\rho_2h_1^2-\rho_1h_2^2] = +1$. (If the sign is negative we can recover Chester's equation by taking $-F$ and by adjusting the time scale by a half-period, π/σ.) If $(\rho_2-\rho_1)/(\rho_1+\rho_2) \leqslant 1$, as is the case in the loch, the symmetry of the solution shows that results for h_2 less than $\frac{1}{2}D$ may be used to infer those for h_2 greater than $\frac{1}{2}D$; that is, in a Boussinesq approximation the profile shapes for $h_2 > h_2$ are the same, but inverted, as those for an upper layer depth equal to h_2 and a lower layer depth equal to h_1.

The solutions of (23) have been examined by Chester, and by Chester & Bones (1968), who present solutions which agree well with their laboratory experiments at the same parameter values. At $x = 0$, one end of the tank, the depth of the lower layer is approximately $h_2 - 2h_1^{(0)}\epsilon_1^{\frac{1}{2}}F(\tau)$. If frequency dispersion and dissipation are both negligible, the last two terms in (23) vanish, and solutions close to resonance exhibit discontinuities, and sudden changes in level are found (see Chester & Bones 1968, figure 4). If $\rho_1h_2^2 > \rho_2h_1^2$, it is found in experiments that

these changes correspond to a fall in level of the interface (Thorpe 1971) consistent with a loss (rather than a gain) in energy at the surge front. They closely resemble the abrupt changes in thermocline level found in Loch Ness (figure 2). The solutions for moderate dispersion and dissipation have the character of an undular bore. The parameter r is a measure of the width of forcing frequency band for which these solutions will be found. If $|r| > 1$ the response is periodic, with little trace of a surge present. Chester's solutions apply to measurements at one end of the tank, but observations in laboratory experiments show that the solutions retain the form they exhibit at the end of the tank even near the centre, although some slight development of the undular wave pattern often accompanies the propagation.

3. The application of the results to Loch Ness

We must first consider how well the model can be applied to the loch, and what values should be chosen for the parameters. The basin which contains the loch (figure 1) is fairly straight and regular in cross-section, although the north-east end is somewhat broader and less regular in shape than the south-west end, and the bottom at the north-east end shelves rather gently, with slopes of about 1:20 in comparison with 1:6 at the south-west end. Some energy is lost from the surge at the north-east end (see figure 3) and the model would be improved by allowing a reduction of the energy of the surge at the ends of the tank. The sides of the basin are remarkably steep, except where rivers enter the loch at Glen Moriston and Glen Urquhart. There is a sill about half-way along the loch caused by the sediment deposited by a small river which enters at Foyers, and here the bottom rises from depths of about 210 m to about 150 m, but still well below the thermocline. The thickness of the thermocline is very small in comparison with the length or width of the basin and with the length of the waves which are observed to follow the surge, but may be as much as half the thickness of the layer above the thermocline. Neither this layer nor the region below the thermocline is isothermal, but contains small temperature gradients. Nevertheless a two-layer model should reproduce the main features of the thermocline movement.

The boundary layers at the bottom and sides of the loch will usually be turbulent. We suppose that the effect may be represented by an eddy viscosity ν with the same value in each layer. We can estimate the mean total rate of dissipation of energy at the boundaries of the loch using the method described by Thorpe (1968*a*, appendix 2) and hence find the e-folding time t_e for a sinusoidal seiche to decay. (We do not account here for the surge, as the values for ν will in any case be only approximate.) We know from the observations of Mortimer (1955) and Thorpe (1971) that t_e is approximately three wave periods, and accounting for dissipation at both the thermocline (as a sharp interface) and at the bottom and sides of the loch, we find a value for an eddy viscosity, $\nu = 11{\cdot}6$ $\mathrm{cm^2\,s^{-1}}$. This we might compare with a value of $26\ \mathrm{cm^2\,s^{-1}}$ found to be suitable in modelling Lake Windermere by Heaps & Ramsbottom (1966).

The presence of the free surface of the loch, rather than the rigid lid assumed in the model, allows surface seiches, but these have periods which are far

removed from the period of the internal surge, and will not interfere.† The effect of having a free top will not significantly modify the shape of the internal waves (Thorpe 1968*a*). Quite ignored in the model is the effect of the rotation of the earth. The consequences of rotation are to modify the natural period of oscillation of the basin (a minor effect for long basins, see Rao 1966), to induce a transverse tilt of the isotherms (Mortimer 1955) and to modify the way in which the wind stress is imparted to water motions by the development of Ekman layers. It is the latter effect which is most difficult to assess. The body force used in the model has no direct counterpart in the loch, although it may represent the effect of the stress on the surface imparted to the region above the thermocline. Some of the stress is however used to generate surface oscillations and circulatory currents in the upper layer, and so only some (unknown) fraction might be considered to be transmitted as an effective body force. In formulating the results we shall take $A_2 = 0$ and $\rho_1 A_1 = q\tau/h_1$, where q is a non-dimensional constant less than unity and τ is the wind stress on the surface of the loch, itself assumed to be uniform and not to vary with position (a sweeping assumption!).

The approximations made in the model itself will be valid provided that the surge is sufficiently weak, and if ϵ, δ, $\epsilon^{\frac{1}{2}}r$ and $\epsilon^{\frac{1}{2}}s$ are small. The current speeds below the thermocline are usually small and much less than the speed of the surge itself, about 37 cm s^{-1}. The motions observed above the thermocline are however often comparable with this speed, but their vertically averaged values are probably small, and only a small change (usually less than 8 cm s^{-1}) is observed as the surge passes. (It is the ratio of this change to the speed of the surge which must be small if approximations made in reducing (7) to (8) are to be valid.)

The model can thus, at best, be only a crude approximation to the loch. With these reservations we estimate the parameters which appear in (23), to see how well the solutions of Chester & Bones and our laboratory experiments (see §4) correspond to the loch, and to examine the range of forcing frequencies for which a surge may develop through resonance. We take $l = 35$ km, $h_1 = 40$ m, $h_2 = 100$ m, $b = 1{\cdot}4$ km and $g(\rho_2 - \rho_1) = 0{\cdot}44$ g^{-2} cm^{-2}, which give $a_0 = 35{\cdot}5$ cm s^{-1} and the natural period $2l/a_0 = 54{\cdot}8$ h. We take a surface stress $\tau = 0{\cdot}16$ dyne cm^{-2}, which is representative of winds near 4 m s^{-1} and hence $\rho_1 A_1 = 4q \times 10^{-5}$ dyne cm^{-3}.

Using these values we find

$$\epsilon = 0{\cdot}080q, \quad \epsilon_1 = 0{\cdot}036q, \quad r = \frac{2{\cdot}9}{q^{\frac{1}{2}}}\left(\frac{\Sigma}{\sigma}\right)\tan\left(\frac{\sigma\pi}{\Sigma}\right), \quad \delta = 9{\cdot}0 \times 10^{-3}, \quad s = \frac{0{\cdot}25}{q^{\frac{1}{2}}}. \tag{24}$$

(We have taken forcing frequencies σ_1 close to the natural frequency $\Sigma = \pi a_0/l$ in calculating ϵ, ϵ_1, δ and s; provided that $|r| < 2$ variations in σ do not produce very large changes from these values. The parameter s is calculated neglecting the action of viscosity on the upper boundary.) The 'constant' q is unknown.

In figure 5 are shown the experimental recordings of surface elevation at $x = 0$ for $\epsilon = 0{\cdot}014$, $\delta = 0{\cdot}065$, $s = 0{\cdot}37$ and at various values of r measured by Chester

† Unless a resonant interaction of the kind described by Smith & Mahony (1972) is possible. The periods of the first three surface seiches are 31·5, 15·3 and 8·8 min (Chrystal 1910).

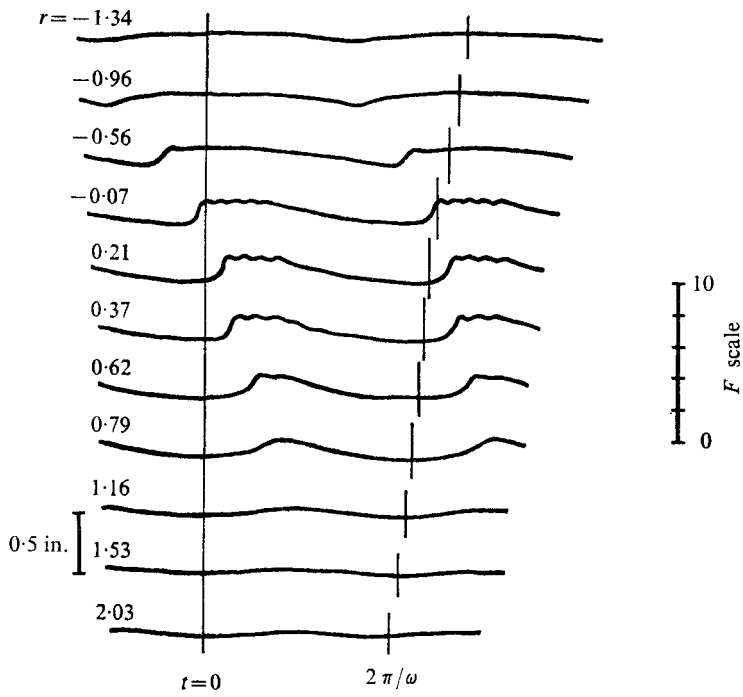

FIGURE 5. Experimental recordings of the surface elevation of the free water surface at one end of a tank, taken from Chester & Bones (1968). The mean depth of water was 0·5 in., and $\epsilon = 0{\cdot}014$, $\delta = 0{\cdot}065$ and $s = 0{\cdot}37$. The elevation is shown at various values of the parameter r.

& Bones (their figure 5; the values of the parameters were kindly communicated to me by Professor Chester). The figure shows very well the abrupt changes in elevation as the surge arrives, and the diminishing response as $|r|$ increases, when the forcing is less well tuned to the natural frequency of the container. The displacement of the interface is equal to $2h\epsilon^{\frac{1}{2}}F(\tau)$, where h is the water depth, 1·27 cm in this experiment. $F(\tau)$ may thus be found from the curves, and on the right we have drawn in the scale for F. If dispersion and dissipation are both neglected F changes by 2 as the surge arrives at the end of the tank when $r = 0$, but in this experiment the change in F is approximately 1·65 near resonance. The corresponding change in the two-layer model is $2h_1\epsilon^{\frac{1}{2}}$ (1·65), or a fraction $0{\cdot}63q^{\frac{1}{2}}$ of the upper layer depth in Loch Ness when we introduce the value of ϵ_1 from (24). In practice changes of 10–20 m are commonly observed in the loch, which give values of q in the range 0·1–0·4. Corresponding ranges of 0·008–0·032 for ϵ and 0·39–0·79 for s are found from (24), close to the values of the parameters in figure 5. Only δ, a measure of the dispersion, is poorly represented by the laboratory experiment, and the changes in isotherm levels in the loch may be expected to be more abrupt than those indicated by figure 5, since the loch value is less than that for the laboratory. A marked surge is found in the laboratory when $|r| < 0{\cdot}5$. For $q = 0{\cdot}25$ in the centre of its range, $|r|$ is less than 0·5 provided that $0{\cdot}949 < \sigma/\Sigma < 1{\cdot}057$. Wind forcing at periods between about 51·8 and 57·7 h

would thus generate a surge. The observed mean period of the surge shown in figure 3 is 56·2 h.

In view of the present uncertainty in calculating the values of the parameters in the loch, it does not seem worth discussing further the other predictions which might be made.

4. Laboratory experiments in a two-layer system: conclusion

The apparatus used for the experiments is one which has been used for a variety of other experiments with stratified fluids (Thorpe 1973). It was not constructed with the present experiments in mind and our ability to model the surge was limited to the parameter range which could be achieved in the existing apparatus. It consists simply of a long rectangular tube with perspex sides and closed ends with a height of 10·0 cm, width 10·25 cm and length 487·5 cm, which can be rocked about a horizontal pivot, like a see-saw. A small vertical oscillation was applied to one end of the tube through a shaft leading from an eccentric cam on a circular disk, which was itself driven by a motor through a hydraulic gearbox. The amplitude of the oscillation about a horizontal position could be varied by adjusting the radial position of the cam on the disk, and the frequency could be changed through the gearbox. The tube was completely filled with two layers of fluid, either paraffin (kerosene) and water, which are immiscible, or brine and water. The interface between the latter fluids was typically 0·8 cm thick when the experiments were begun.

The effect of rocking the tube through a small angle α is equivalent to applying a periodic body force $g\alpha$ per unit mass, and thus

$$\rho_1 A_1 - \rho_2 A_2 = g\alpha(\rho_2 - \rho_1)$$

(taken positive by definition). With this identification the experiment corresponds closely to the model described by the theory. When oscillation was begun at a frequency close to the natural frequency Σ a surge front quickly developed, reaching a constant amplitude after about four periods. Figure 6 (plate 1) shows the appearance of the front of the surge at the interface between brine and water as it approached the right-hand end of the tube. The parameters are given in the figure caption, and the experiment has been arranged so that they correspond approximately to the parameters expected in Loch Ness. The experiments reproduce the depression of the thermocline as the surge passes, and the undular form of the surge. The period of the waves in the loch is however relatively smaller, by about half, than of those in the laboratory. This is probably in part the result of poor modelling of the parameter δ; the thickness of the thermocline may also be important.

The wave trains which followed the front of the surge were much longer in extent in the experiments with a diffuse interface between brine and water than in those with a sharp interface between immiscible fluids, presumably owing to enhanced viscous dissipation in the latter. Several effects not accounted for in the theory were observed when the forcing amplitude was sufficiently increased. Rippling, or billow formation, evidence of shear instability, was observed near the leading

wave crest (or trough for surges in which the interface was lowered). In the experiments with brine and water non-stationary 'cusped waves' of the kind described by Thorpe (1973) were observed in front of the surge. These are thought to be caused by shear instability in a transition region in which the velocity interface is thicker than the density interface. Near the ends of the tube the short waves following the surge produced a standing-wave pattern during the reflexion of the surge, with breaking occurring at the wave nodes in the manner described in earlier experiments (Thorpe 1968*a*). These short waves are fairly regular close to the front of the surge but become irregular after the first four or five waves, with higher harmonics establishing themselves. This is possibly due to a second-order resonance phenomenon of the kind described by Davis & Acrivos (1967). A side-band instability of the kind discussed by Benjamin & Feir (1967) for surface waves is unlikely to occur in the loch (see appendix B). A note about the shape of the waves which follow the surge is included in appendix C.

These observations suggest that some of the irregularities which follow the leading waves of the surge in Loch Ness are not due entirely to reflexions at the sides of the loch or to other externally induced disturbances, but may result from interactions in the wave train itself.

It is remarkable that large surges are most commonly observed in Loch Ness in early October. We at first thought that this might be due to the fact that at this season the thermocline depth is such that the natural period of the Loch is close to 48 h, and that a parametric resonance with the wind, which often has a notable diurnal component due to sea breezes, might be possible. In Seneca Lake, however, which has a natural period of about 77 h, Hunkins & Fliegel have also noticed that the largest and most frequent surges are in October, although no positive correlation with winds is available. A factor which may be important is the thickness of the thermocline, but an investigation is beyond the scope of this paper. The greatest uncertainty in the present model of the forced motion of the loch is that of properly accounting for the wind stress, and the effect which it has on the loch. Recent experiments have been made to observe the development of drift currents in the loch when the wind increases, and to investigate the effect which the wind has on the stratification, and it is hoped that a more satisfactory model may eventually be formulated.

I am grateful to the members of the staff of the I.O.S. who have made the observations in Loch Ness possible, and particularly to Mr Alan Hall for constructing and operating the instruments and for his assistance both in analysing the data and in making the laboratory experiments.

Appendix A

When the dispersive and dissipative effects are substantial, and terms of higher order than the first are omitted in the expressions for dispersion and dissipation, equation (8) becomes, correct to second order,

$$\rho_1 \frac{\partial u_1^{(2)}}{\partial t} - \rho_2 \frac{\partial u_2^{(2)}}{\partial t} - g(\rho_2 - \rho_1) \frac{\partial h_2^{(2)}}{\partial x}$$

$$= \rho_2 u_2^{(1)} \frac{\partial u_2^{(1)}}{\partial x} - \rho_1 u_1^{(1)} \frac{\partial u_1^{(1)}}{\partial x}$$

$$- a_0^2 \frac{(\rho_1 h_1^{(0)} + \rho_2 h_2^{(0)})}{\pi h_2^{(0)3}} \int_{-\infty}^{\infty} \frac{\partial}{\partial x} [h_2^{(1)}(x-\zeta, t) - h_2^{(1)}(x,t)] \log \tanh \frac{\pi|\zeta|}{4h_2^{(0)}} \, d\zeta$$

$$- 2\left(\frac{\nu_1}{\pi}\right)^{\frac{1}{2}} \rho_1 \left(\frac{1}{b} + \frac{1}{h_1^{(0)}}\right) \int_0^{\infty} \frac{\partial u_1^{(1)}}{\partial t}(x, t-\zeta) \zeta^{-\frac{1}{2}} \, d\zeta$$

$$+ 2\left(\frac{\nu_2}{\pi}\right)^{\frac{1}{2}} \rho_2 \left(\frac{1}{b} + \frac{1}{h_2^{(0)}}\right) \int_0^{\infty} \frac{\partial}{\partial t} u_2^{(1)}(x, t-\zeta) \zeta^{-\frac{1}{2}} \, d\zeta, \tag{A 1}$$

whilst (1) becomes

$$\frac{\partial h_2^{(2)}}{\partial t} + h_2^{(0)} \frac{\partial u_2^{(2)}}{\partial x} = - h_2^{(1)} \frac{\partial u_2^{(1)}}{\partial x} \tag{A 2}$$

and (2) becomes

$$h_1^{(0)} u_1^{(2)} + h_2^{(0)} u_2^{(2)} = - h_1^{(1)} u_1^{(1)} - h_2^{(1)} u_2^{(1)}. \tag{A 3}$$

We let

$$U = \gamma_1 u_1^{(2)} + \gamma_2 u_2^{(2)}, \tag{A 4}$$

where γ_1 and γ_2 are constants, and obtain expressions for $u_1^{(2)}$ and $u_2^{(2)}$ in terms of U from (A 3) and (A 4). When these are substituted into (A 1) and (A 2) we find

$$\frac{\partial U}{\partial t} + a_0 \frac{\partial h_2^{(2)}}{\partial x} = - \frac{h_1^{(0)} h_2^{(0)}}{a_0(\rho_1 h_2^{(0)} + \rho_2 h_1^{(0)})} \chi - \frac{\rho_1 \gamma_2 + \rho_2 \gamma_1}{\rho_1 h_2^{(0)} + \rho_2 h_1^{(0)}} \frac{\partial}{\partial t}(h_1^{(1)} u_1^{(1)} + h_2^{(1)} u_2^{(1)}) \tag{A 5}$$

and

$$\frac{\partial h_2}{\partial t} + a_0 \frac{\partial U}{\partial x} = - h_2^{(1)} \frac{\partial u_2^{(1)}}{\partial x} - \frac{\gamma_1 a_0}{h_0} \frac{\partial}{\partial x}(h_1^{(1)} u_1^{(1)} + h_2^{(1)} u_2^{(1)}), \tag{A 6}$$

where

$$h_1^{(0)} \gamma_2 - h_2^{(0)} \gamma_1 = h_1^{(0)} h_2^{(0)} / a_0, \tag{A 7}$$

and χ is equal to the terms appearing on the right-hand side of (A 1). Adding and subtracting (A 5) and (A 6), and substituting the expressions for $h_1^{(1)}$, $h_2^{(1)}$, $u_1^{(1)}$ and $u_2^{(1)}$ from (13)–(15) but only including the dominant terms near resonance, we find

$$\left(\frac{\partial}{\partial t} \pm a_0 \frac{\partial}{\partial x}\right)(U + h_2^{(2)})$$

$$= \frac{(\rho_1 h_2^{(0)2} - \rho_2 h_1^{(0)2}) h_1^{(0)}}{a_0^2 h_2^{(0)}(\rho_1 h_2^{(0)} + \rho_2 h_1^{(0)})} (f_+' + f_-')(f_+ - f_-) - \frac{2(\rho_2 \gamma_1 - \rho_1 \gamma_2) a_0 (h_1^{(0)} + h_2^{(0)}) h_1^{(0)}}{h_2^{(0)}(\rho_1 h_2^{(0)} + \rho_2 h_1^{(0)})}$$

$$\times (f_+ f_+' - f_- f_-') \pm \frac{2a_0^2}{\sigma^2 h_2^{(0)}} (f_+ f_+' + f_- f_-') \left[1 + \frac{\gamma_1 a_0 (h_1^{(0)} + h_2^{(0)})}{h_1^{(0)}}\right]$$

$$+ \frac{h_1^{(0)2}}{\pi h_2^{(0)2}} \int_{-\infty}^{\infty} \left[f'\left(t + \frac{x}{a_0} - \frac{\zeta}{a_0}\right) - f'\left(t - \frac{x}{a_0} + \frac{\zeta}{a_0}\right) - f'\left(t + \frac{x}{a_0}\right) + f'\left(t - \frac{x}{a_0}\right)\right]$$

$$\times \log\tanh\frac{\pi|\zeta|}{4h_2^{(0)}}\,d\zeta+\frac{2h_1^{(0)2}h_2^{(0)}}{\rho_1h_2^{(0)}+\rho_2h_1^{(0)}}\left[\left(\frac{\nu_1}{\pi}\right)^{\frac{1}{2}}\rho_1\left(\frac{1}{b}+\frac{1}{h_1^{(0)}}\right)\frac{1}{h_1^{(0)}}\right.$$
$$\left.+\left(\frac{\nu_2}{\pi}\right)^{\frac{1}{2}}\rho_2\left(\frac{1}{b}+\frac{1}{h_2^{(0)}}\right)\frac{1}{h_2^{(0)}}\right]\int_0^\infty\left[f'\left(t-\zeta-\frac{x}{a_0}\right)-f'\left(t-\zeta+\frac{x}{a_0}\right)\right]\zeta^{-\frac{1}{2}}\,d\zeta, \tag{A 8}$$

where $f_+\equiv f(t+x/a_0)$, $f_-\equiv f(t-x/a_0)$, $f'_+=df(\eta)/d\eta$ evaluated at $\eta=t+x/a_0$, etc. The equations have the following particular solutions:

$$U\pm h_2^{(2)}=\frac{(\rho_1h_2^{(0)2}-\rho_1h_1^{(0)2})\,h_1^{(0)}}{a_0^2h_2^{(0)}(\rho_1h_2^{(0)}+\rho_2h_1^{(0)})}\left[\pm f_\pm^2-\frac{x}{a_0}f_\mp f'_\mp\mp\tfrac{1}{2}f_+f_-\pm\tfrac{1}{2}f'_\mp I_\pm\right]$$
$$-\frac{2(\rho_2\gamma_1-\rho_1\gamma_2)\,a_0(h_1^{(0)}+h_2^{(0)})\,h_1^{(0)}}{h_2^{(0)}(\rho_1h_2^{(0)}+\rho_2h_1^{(0)})}\left[\pm\tfrac{1}{4}f_\pm^2-\frac{x}{a_0}f_\mp f'_\mp\right]$$
$$+\frac{2h_1^{(0)}}{h_2^{(0)}}\left[1+\frac{\gamma_1a_0}{h_1^{(0)2}}(h_1^{(0)}+h_2^{(0)})\right]\left[\frac{x}{a_0}f_\mp f'_\mp\pm\tfrac{1}{4}f_\pm^2\right]$$
$$+\frac{h_1^{(0)2}}{\pi a_0h_2^{(0)2}}\int_{-\infty}^{\infty}\left\{\pm\tfrac{1}{2}a_0f\left(t\pm\frac{x}{a_0}\mp\frac{\zeta}{a_0}\right)-xf'\left(t\mp\frac{x}{a_0}\pm\frac{\zeta}{a_0}\right)\mp\tfrac{1}{2}a_0f_\pm+xf'_\mp\right\}$$
$$\times\log\tanh\left(\frac{\pi|\zeta|}{4h_2^{(0)}}\right)d\zeta+\frac{2h_1^{(0)2}h_2^{(0)}}{a_0(\rho_1h_2^{(0)}+\rho_2h_1^{(0)})}\left[\left(\frac{\nu_1}{\pi}\right)^{\frac{1}{2}}\rho_1\left(\frac{1}{b}+\frac{1}{h_1^{(0)}}\right)\frac{1}{h_1^{(0)}}\right.$$
$$\left.+\left(\frac{\nu_2}{\pi}\right)^{\frac{1}{2}}\rho_2\left(\frac{1}{b}+\frac{1}{h_2^{(0)}}\right)\frac{1}{h_2^{(0)}}\right]\int_0^\infty\left\{\pm\frac{a_0}{2}f\left(t-\zeta\pm\frac{x}{a_0}\right)-xf'\left(t-\zeta\mp\frac{x}{a_0}\right)\right\}\zeta^{-\frac{1}{2}}\,d\zeta, \tag{A 9}$$

where
$$I_\pm\equiv I\left(t\pm\frac{x}{a_0}\right)=\int^{t\pm x/a_0}f(\eta)\,d\eta.$$

Appendix B. 'Side-band' interactions in a two-layer fluid

It has been shown by Whitham (1967) that progressive waves of frequency σ, wavenumber k and amplitude A such that

$$\sigma=\sigma_0(k)+k^2A^2\sigma_2(k)+\text{terms of higher powers of } A$$

are unstable, finding resonances and interacting with waves which have frequencies close to σ, if

$$\chi\equiv(\partial^2\sigma_0/\partial k^2)\,\sigma_2<0.$$

No such resonances are possible if $\chi>0$. For example, the dispersion relation for surface waves in deep water is

$$\sigma=(gk)^{\frac{1}{2}}(1+\tfrac{1}{2}k^2A^2),$$

neglecting higher order terms, and $\chi=-g/8k<0$, and the waves are found experimentally to be unstable (Benjamin & Feir 1967), transferring their energy to side bands.

The dispersion relation for progressive internal waves in a two-layer fluid is given by

$$\sigma_0^2=gk(\rho_2-\rho_1)t_1t_2/(\rho_1t_2+\rho_2t_1),$$
$$\sigma_2=\frac{\sigma_0t_1t_2}{4(\rho_1t_2+\rho_2t_1)}\left\{\frac{\rho_1}{t_1^3}(2t_1^2-1)+\frac{\rho_2}{t_2^3}(2t_2^2-1)+\frac{1}{4(\rho_1t_1+\rho_2t_2)}\left[\frac{\rho_2}{t_2^2}(3-t_2^2)-\frac{\rho_1}{t_1^2}(3-t_1^2)\right]\right\}$$

(Thorpe 1968*a*), where $t_1 = \tanh kh_1$, $t_2 = \tanh kh_2$, and ρ_1, ρ_2, h_1 and h_2 are defined as before. It is easy to show that for waves with $kh_1 = 0{\cdot}25$ and $kh_2 = 0{\cdot}63$, typical of the waves which follow the front of the surge in Loch Ness,

$$\partial^2\sigma_0/\partial k^2 > 0, \quad \sigma_2 > 0,$$

and so the waves are stable to side-band disturbances. The waves following the surge shown in figure 6 (plate 1) are also such that $\chi > 0$ and are therefore stable. However waves typical of the ocean thermocline, when h_2 is very large and $t_2 = 1$, $\rho_2 - \rho_1 \ll \rho_2$, are such that

$$\partial^2\sigma_0/\partial k^2 < 0, \quad \sigma_2 > 0$$

and so are unstable to side-band instabilities.

This is, however, an interaction in which energy is transferred at third order, and it is more probable that resonant interactions at second order (Davis & Acrivos 1967) will occur in practice.

Appendix C. A note on the shape of waves in a two-layer shear flow

It has been shown (Thorpe 1968*b*) how short waves in a two-layer fluid with no Eulerian mean flow in either layer and with a small density difference between the layers have crests which are narrower than their troughs if the lower layer is shallow and the upper is deep. Their shape is similar to that of surface waves. The troughs are narrower than the crests if the upper layer is the shallower. The object of this note is to point out that this result may not be true if the mean flow is non-zero.

Consider for example a density front which advances with a wave train behind it into still water at speed c. The wave train is stationary with respect to the front. We take a frame of reference in which the waves, and the lower fluid, are at rest, with the upper layer, which for example we suppose is of infinite depth, moving past with a mean speed c. If ϕ is the velocity potential in the upper layer and η is the interface displacement, then the motion is described by the Laplace equation,

$$\nabla^2\phi = 0,$$

with the boundary conditions

$$\frac{D\eta}{Dt} = \frac{\partial\phi}{\partial z}, \quad \frac{1}{2}\left[\left(\frac{\partial\phi}{\partial x}\right)^2 + \left(\frac{\partial\phi}{\partial z}\right)^2\right] + g\eta\left(1 - \frac{\rho_2}{\rho_1}\right) = \text{constant at } z = \eta,$$

$$\partial\phi/\partial x \to c, \quad \partial\phi/\partial z \to 0 \quad \text{as} \quad z \to \infty.$$

These equations are exactly those of waves on the free surface of a deep fluid in a gravitational field

$$g' = g(\rho_2 - \rho_1)/\rho_1$$

directed upwards, as can be seen if the sign of z is reversed. Thus the shape of the interfacial waves is the same as those at the free surface of a deep layer, but inverted, so that their troughs are narrower than their crests.

This is just the opposite of the result found before. The waves which are observed to follow the surge in the laboratory experiment with a shallow upper layer are sometimes shaped like surface waves.

REFERENCES

BENJAMIN, T. B. & FEIR, J. E. 1967 *J. Fluid Mech.* **27**, 417–430.

CAVANIE, A. G. 1971 *Cahiers Oceanog.* **23**, 611–627.

CHESTER, W. 1968 *Proc. Roy. Soc.* A **306**, 5–22.

CHESTER, W. & BONES, J. A. 1968 *Proc. Roy. Soc.* A **306**, 23–39.

CHRYSTAL, G. 1910 *Bathymetrical Survey of the Scottish Fresh-Water Lakes* (ed. Murrey & Puller), vol. 1, pp. 29–90. Edinburgh: Challenger Office.

DAVIS, R. E. & ACRIVOS, A. 1967 *J. Fluid Mech.* **30**, 723–736.

GARGETT, A. E. & HUGHES, B. A. 1972 *J. Fluid Mech.* **52**, 179–192.

HALPERN, D. 1971 *J. Mar. Res.* **29**, 116–132.

HEAPS, N. S. & RAMSBOTTOM, A. E. 1966 *Phil. Trans.* A **259**, 391–430.

HUNKINS, K. & FLIEGEL, M. 1973 *J. Geophys. Res.* **79**, 539–548.

LONG, R. R. 1972 *Tellus*, **24**, 88–99.

MORTIMER, C. H. 1955 *Proc. Intern. Assoc. Appl. Limnol.* **12**, 66–77.

RAO, D. B. 1966 *J. Fluid Mech.* **25**, 523–555.

SMITH, R. & MAHONY, J. J. 1972 *J. Fluid Mech.* **53**, 193–207.

THORPE, S. A. 1968*a* *J. Fluid Mech.* **32**, 489–528.

THORPE, S. A. 1968*b* *Phil. Trans.* A **263**, 563, 614.

THORPE, S. A. 1971 *Nature*, **231**, 306–308.

THORPE, S. A. 1973 *Bdry-Layer Meteorol.* **5**, 95–119.

THORPE, S. A., HALL, A. & CROFTS, I. 1972 *Nature*, **237**, 96–98.

WATSON, E. R. 1904 *Geog. J.* **24**, 430–437.

WEDDERBURN, E. M. 1907 *Trans. Roy. Soc. Edin.* **45**, 407–489.

WEDDERBURN, E. M. 1911 *Trans. Roy. Soc. Edin.* **48**, 629–695.

WHITHAM, G. B. 1967 *J. Fluid Mech.* **27**, 399–412.

ZIEGENBEIN, J. 1969 *Deep-Sea Res.* **16**, 479–487.